# Elementary Steps in the Reaction of Horseradish Peroxidase with Several Peroxides: Kinetics and Thermodynamics of Formation of Compound 0 and Compound I[†]

## Haesun K. Baek and Harold E. Van Wart*

*Contribution from the Department of Chemistry and Institute of Molecular Biophysics, Florida State University, Tallahassee, Florida 32306. Received May 24, 1991*

**Abstract:** The reactions of horseradish peroxidase (HRP) with ethyl hydroperoxide, *tert*-butyl hydroperoxide, and peracetic acid to form compound I have been studied in 50% v/v methanol/10 mM phosphate over the +25 to −35 °C temperature range using the low-temperature stopped-flow technique. All reactions were carried out under pseudo-first-order conditions with [peroxide] $\gg$ [HRP]. Arrhenius plots for $k_{obs}$ obtained under conditions where [peroxide] $\ll K_M$ are linear over the entire temperature range studied for each reaction, indicating that there is no change in mechanism over this temperature range. Above 0 °C, the pseudo-first-order rate constant for compound I formation, $k_{obs}$, varies linearly with [peroxide] for each reaction. However, saturation kinetics are observed below −16 °C for all of these reactions, indicating that they proceed via at least one reversible elementary step involving the formation of an intermediate. Rapid-scan optical studies have been carried out at −35 °C at [peroxide] $\gg K_M$ for each reaction in order to record the optical spectrum of the intermediate. In all three reactions, the Soret region of the intermediate exhibits bands near 360 and 410 nm and there is a weak band in the visible near 570 nm. These are the same spectral features that have been observed earlier for compound 0, an intermediate in the reaction of HRP with hydrogen peroxide. Thus, the compound I formation reaction is viewed as at least a two-step process. Double reciprocal plots obtained over the −20 to −30 °C range at pH* 7.3 for these reactions give values of $K_M^{-1}$ and $k_{obs}^{max}$ that reflect the formation of compound 0 and its rate of conversion to compound I, respectively. The values of $k_{obs}^{max}$ are not strongly dependent on the identity of the peroxide. However, the values of $K_M^{-1}$ decrease markedly for the bulkier peroxides. Possible structures for compound 0 are discussed.

## Introduction

The initial step in the mechanism of action of all of the hydroperoxidases is their interaction with $H_2O_2$. Most of these enzymes are ferric heme species, and all react with $H_2O_2$ to form a catalytically active reaction intermediate that is referred to as compound I.[1-3] This reaction is characterized by the reduction of $H_2O_2$ to $H_2O$ and the concomitant two-electron oxidation of the enzyme. The sites of this oxidation vary from one hydroperoxidase to another. All of these enzymes appear to store one oxidizing equivalent in the form of an oxyferryl species. However, the second equivalent can be stored as an $^2A_{2u}$ (e.g., horseradish peroxidase) or $^2A_{1u}$ (e.g., catalase) $\pi$-cation porphyrin radical, on an amino acid residue of the protein (e.g., cytochrome c peroxidase), or on another redox-active heme cofactor (e.g., *Pseudomonas aeruginosa* cytochrome $c_{551}$ peroxidase).[3] In order to understand the diverse consequences of this reaction in the different hydroperoxidases, a detailed picture of the mechanism of compound I formation is desirable.

Attempts to study the elementary steps in the compound I formation reaction have been frustrated by the inability of conventional stopped-flow experiments to monitor the reaction at high enough $[H_2O_2]$ to reveal the presence of intermediates,[3] even though the existence of at least one intermediate has been predicted from other data.[4] This is a common limitation in the study of essentially irreversible fast reactions, and the low-temperature stopped-flow technique has been developed to expand the range of study of such reactions.[5-7] In an earlier report, it was demonstrated that this technique permitted the study of the reaction of horseradish peroxidase (HRP) with high enough $[H_2O_2]$ in 50% v/v methanol/10 mM phosphate that saturation kinetics could be observed below −16 °C.[8] Thus, this reaction pathway contains at least one reversible step that is the formation of a precursor to compound I that was referred to as compound 0. The optical spectrum of this new intermediate was observed directly in rapid-scan experiments and found to exhibit a characteristic band in the Soret region near 330 nm.

A knowledge of the structure of HRP compound 0 would be invaluable in revealing details of the initial interaction between

HRP and $H_2O_2$ that ultimately leads to the formation of compound I. Until it can be stabilized and subjected to study by techniques capable of providing this structural information, however, it is of interest to complete any kinetic measurements that would help characterize this new species. In this paper, we present a low-temperature stopped-flow investigation of the reaction of HRP with three other hydroperoxides, $RO_2H$, in order to assess whether a compound 0 is present in these reactions. In particular, measurements at different temperatures are made in order to characterize the reaction pathways both kinetically and thermodynamically. This study also examines the validity of another report[9] which describes low-temperature stopped-flow studies of the reaction between HRP and two peroxides.

## Experimental Procedures

**Materials.** HRP (EC 1.11.1.7) isozyme C was purchased from Sigma Chemical Co. as a salt-free lyophilized powder (type VI) and used without further purification. The ratio of absorbance at 403 to 280 nm was above 3.0. Reagent grade $H_2O_2$ (30% v/v) was obtained from J. T. Baker Chemical Co., ethyl hydroperoxide ($EtO_2H$) from Polysciences, Inc., *tert*-butyl hydroperoxide ($t$-$BuO_2H$) from Sigma Chemical Co., and peracetic acid ($AcO_2H$) from Aldrich. Spectranalyzed methanol and dimethyl sulfoxide (DMSO) were purchased from Fisher Scientific. All buffer solutions were made from reagent grade water with a resistivity of 18 MΩ/cm that was prepared with a Millipore Milli-Q system. The concentrations of HRP,[10] $H_2O_2$,[11] and $EtO_2H$[12] were determined spectrophotometrically by using $\epsilon_{403} = 1.02 \times 10^5$ $M^{-1}$ $cm^{-1}$, $\epsilon_{240} = 39.4$ $M^{-1}$

(1) Dunford, H. B.; Stillman, J. S. *Coord. Chem. Rev.* **1976**, *19*, 197–251.
(2) Hewson, W. D.; Hager, L. P. In *The Porphyrins*; Dolphin, D., Ed.; Academic: New York, 1979; Vol. VII, pp 295–332.
(3) Frew, J. E.; Jones, P. In *Advances in Inorganic and Bioinorganic Mechanisms*; Sykes, A. G., Ed.; Academic: New York, 1984; Vol. 3, pp 175–212.
(4) Jones, P.; Dunford, H. B. *J. Theor. Biol.* **1977**, *69*, 457–470.
(5) Hui Bon Hoa, G.; Douzou, P. *Anal. Biochem.* **1973**, *51*, 127–136.
(6) Hanahan, D.; Auld, D. S. *Anal. Biochem.* **1980**, *108*, 86–95.
(7) Van Wart, H. E.; Zimmer, J. *Anal. Biochem.* **1981**, *117*, 410–418.
(8) Baek, H. K.; Van Wart, H. E. *Biochemistry* **1989**, *28*, 5714–5719.
(9) Balny, C.; Travers, F.; Barman, T.; Douzou, P. *Eur. Biophys. J.* **1987**, *14*, 375–383.
(10) Schonbaum, G. R.; Lo, S. *J. Biol. Chem.* **1972**, *247*, 3353–3360.
(11) Nelson, D. P.; Kieson, L. A. *Anal. Biochem.* **1972**, *49*, 474–478.
(12) Swern, O., Ed. *Organic Peroxides*; Wiley: New York, 1971; Vol. 1, p 209.
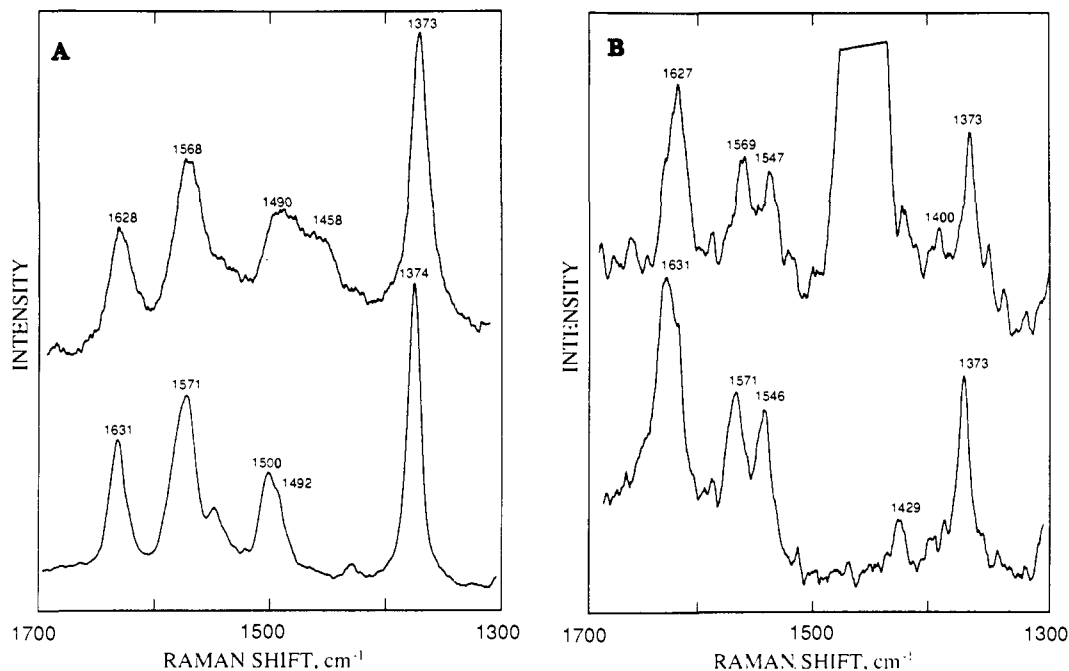
**Figure 1.** Resonance Raman spectra of HRP dissolved in 10 mM phosphate in the presence (top spectra) and absence (bottom spectra) of 50% v/v methanol at pH (or pH*) 7.3, 23 °C, excited at (A) 413.1 and (B) 514.5 nm. Spectra were recorded with a power at the sample of 10–30 mW and an instrumental resolution of 5 cm$^{-1}$ at HRP concentrations of (A) 20 and (B) 100 $\mu$M.

cm$^{-1}$, and $\epsilon_{230}$ = 43 M$^{-1}$ cm$^{-1}$, respectively. The concentrations of AcO$_2$H and $t$-BuO$_2$H were measured by iodometric titration with sodium thiosulfate. The small quantities of H$_2$O$_2$ that contaminate solutions of EtO$_2$H, $t$-BuO$_2$H, and AcO$_2$H were decomposed by addition of a trace of catalase before their use.

**Low-Temperature Stopped-Flow Experiments.** The low-temperature stopped-flow experiments were carried out with an instrument described elsewhere[7] which contains an observation cell with a path length of 2 cm. For single wavelength measurements, more than 200 data points were used in each rate constant determination. The reported rate constants are the average of at least three trials. The rapid-scan spectra were acquired by focusing light from an Oriel 75-W xenon lamp attenuated with a neutral density filter with a quartz lens through the observation cell of the stopped-flow instrument and into a Princeton Applied Research Model 1226 spectrograph. The light is dispersed and focused onto a home-built diode array detector constructed from a Hamamatsu Model S2304-512Q linear silicon photodiode array sensor interfaced to a MicroWay A2D-160 12-bit 166-kHz analog-to-digital converter.[13] The selection of integration time was controlled by software written by us for this instrument. The wavelength calibration of the diode array was achieved using the lines from a mercury lamp.

All stopped-flow measurements were performed under pseudo-first-order conditions with [peroxide] $\geq$ 10[HRP], and values of the pseudo-first-order rate constant, $k_{obs}$, were obtained from fits to the exponential change in absorbance at 397 nm. Experiments were carried out at [HRP] of both 1.0 and 7.0 $\mu$M. The cryosolvents used in all of the low-temperature stopped-flow experiments were 50% v/v methanol/buffer or 60% v/v DMSO/buffer, where the buffer was either 10 mM phosphate or 40 mM Tris. The apparent protonic activity in these cryosolvents, pH*, at subzero temperatures was estimated from tables of the temperature dependence of their pH* values,[14] as described elsewhere.[15] A minimum of 1 h was allowed for temperature equilibrium to occur before kinetic runs were initiated. The temperature of the stopped-flow system was monitored throughout all experiments with an Omega copper/constantan grounded thermocouple and an Omega Model 2176 A-T digital thermometer.

**Resonance Raman Experiments.** Resonance Raman spectra of HRP were obtained with a SPEX Model 1403 Raman spectrometer using excitation from the 413.1 and 514.5 nm lines of Spectra Physics Model 2020 krypton ion and Coherent Radiation Innova Model 90 argon ion lasers, respectively, as described elsewhere.[16]

## Results

**Effect of Components of the Cryosolvent on the Structure and Reactivity of HRP.** The cryosolvent chosen for use in any cryoenzymological study should serve only to solubilize the reactants and act as a medium for the reaction, but not appreciably inhibit the enzyme, alter its conformation, or change the reaction pathway compared to that in aqueous solution. The choice of 50% v/v methanol/10 mM phosphate as the cryosolvent for the studies described here was based on its high dielectric constant, low freezing point, moderate viscosity, small temperature dependence of pH*, and successful use with HRP in previous studies.[7,8,14,17] It was demonstrated earlier[8] that this cryosolvent lowers the $k_{obs}$ value for the reaction of HRP with H$_2$O$_2$ to form compound I by only 3.5-fold compared to the aqueous reaction over the entire 5.5–9.0 pH* range at 23 °C and gives a linear Arrhenius plot for $k_{obs}$ from +17.6 to –36 °C. Additional evidence that this cryosolvent does not alter the structure or environment of the heme group of HRP comes from resonance Raman experiments. Spectra of HRP in 10 mM phosphate, pH 7.3, and 50% v/v methanol/10 mM phosphate, pH* 7.3, obtained with both Soret-band (413.1 nm) and Q-band (514.5 nm) excitation are shown in Figure 1. The frequencies of the porphyrin skeletal stretching bands shown in these two sets of spectra provide information about the oxidation state, coordination number, and spin state of the heme group.[18] In the absence of methanol, HRP exhibits bands $\nu_4$ and $\nu_2$ at 1374 and 1571 cm$^{-1}$ (Figure 1A) and bands $\nu_{10}$, $\nu_{19}$, and $\nu_{11}$ at 1631, 1571, and 1546 cm$^{-1}$ (Figure 1B), respectively. These catalog most closely with a predominantly five-coordinate, high-spin ferric heme.[19] In the presence of methanol, the spectra are substantially the same with $\nu_{10}$, $\nu_2$, $\nu_{19}$, $\nu_{11}$, and $\nu_4$ bands at 1627, 1568, 1569, 1547, and 1373 cm$^{-1}$, respectively. The new band in the 1450–1500-cm$^{-1}$ region is due to methanol. In particular, there is no evidence for six-coordinate high-spin or low-spin species. Thus, methanol is not coordinated to the sixth site of the heme group of HRP in 50% v/v methanol solutions, nor are any other marked alterations in structure suggested from these spectra.

(13) Carter, T. P.; Baek, H. K.; Bonninghausen, L.; Morris, R. J.; Van Wart, H. E. *Anal. Biochem.* **1990**, *190*, 134–140.

(14) Douzou, P. *Cryobiochemistry: An Introduction*; Academic: New York, 1977; pp 11–90.

(15) Lin, W.-Y.; Lin, S. H.; Morris, R. J.; Van Wart, H. E. *Biochemistry* **1988**, *27*, 5068–5074.

(16) Chuang, W.-J.; Johnson, S.; Van Wart, H. E. *J. Inorg. Biochem.* **1988**, *34*, 201–219.

(17) Van Wart, H. E.; Zimmer, J. *J. Biol. Chem.* **1985**, *260*, 8372–8377.

(18) Spiro, T. G. In *Iron Porphyrins, Part II*; Lever, A. B. P., Gray, H. B., Eds.; Addison-Wesley: Reading, MA, 1983; pp 89–159.

(19) Evangelista-Kirkup, R.; Crisanti, M.; Poulos, T. L.; Spiro, T. G. *FEBS Lett.* **1985**, *190*, 221–226.

**Table I.** Effect of Experimental Conditions on the Kinetic Parameters for the Reaction of HRP with $H_2O_2$ and $EtO_2H$ To Form Compound I in 50% v/v Methanol/Buffer Solutions

| peroxide | buffer | pH* | [HRP] ($\mu$M) | $T$ (°C) | $k_{obs}^{max}$ (s$^{-1}$) | $K_M$ (mM) | ref |
|---|---|---|---|---|---|---|---|
| $H_2O_2$ | 10 mM phosphate | 7.3 | 1.0 | -26.0 | 163 | 0.190 | 8 |
| $H_2O_2$ | 10 mM phosphate | 9.0 | 1.0 | -26.0 | 204 | 0.235 | 8 |
| $H_2O_2$ | 40 mM Tris | 7.5 | 1.0 | -26.0 | 164 | 0.162 | this study |
| $H_2O_2$ | 40 mM Tris | 9.4 | 1.0 | -31.0 | 188 | 0.310 | this study |
| $H_2O_2$ | 40 mM Tris | 9.3 | 6.0 | -29.4 | 202 | 0.256 | this study |
| $H_2O_2$ | 40 mM Tris | 8.7 | 6.5 | -29.5 | 330 | 1.1 | 9 |
| $EtO_2H$ | 10 mM phosphate | 7.3 | 1.0 | -28.8 | 157 | 2.61 | this study |
| $EtO_2H$ | 10 mM phosphate | 9.1 | 1.0 | -29.0 | 176 | 2.88 | this study |
| $EtO_2H$ | 40 mM Tris | 9.4 | 1.0 | -29.0 | 151 | 2.45 | this study |
| $EtO_2H$ | 40 mM Tris | 9.3 | 6.0 | -29.0 | 156 | 2.82 | this study |
| $EtO_2H$ | 40 mM Tris | 8.7 | 6.5 | -29.5 | 28 | 0.71 | 9 |

Balny and co-workers have also published a low-temperature stopped-flow study of the reaction of HRP with $H_2O_2$ and $EtO_2H$.[9] Some of their experiments were carried out in 50% v/v methanol/40 mM Tris, pH* 8.7, and others in 60% v/v DMSO/40 mM Tris, pH* 8.7. The kinetic parameters reported by these researchers for the reaction of HRP with $H_2O_2$ in the first cryosolvent are in only fair agreement with those reported by us earlier[8] and those for the reaction with $EtO_2H$ to be reported below. For the reaction with $H_2O_2$, our parameters measured in 50% v/v methanol/10 mM phosphate at pH* 9.0 at -26 °C using a [HRP] = 1.0 $\mu$M are $k_{obs}^{max}$ = 204 s$^{-1}$ and $K_M$ = 0.235 mM, while those of Balny and associates measured in 50% v/v methanol/40 mM Tris, pH* 8.7, at -29.5 °C using [HRP] = 6.5 $\mu$M were $k_{obs}^{max}$ = 330 s$^{-1}$ and $K_M$ = 1.1 mM.[9]

In order to assess whether these differences were the result of the slightly different conditions used, the effects of using 40 mM Tris vs 10 mM phosphate, of using [HRP] = 6.5 vs 1.0 $\mu$M, and of using -29.5 vs -26.0 °C in the determination of the $k_{obs}^{max}$ and $K_M$ values for the reaction of HRP with $H_2O_2$ and $EtO_2H$ in 50% v/v methanol/buffer were investigated (Table I). Changing these conditions either individually or collectively has only a small effect on the kinetic parameters. In experiments carried out under conditions almost identical to those reported by Balny and associates,[9] their $k_{obs}^{max}$ value of 330 s$^{-1}$ is in reasonable agreement with ours of 202 s$^{-1}$, but their $K_M$ value of 1.1 mM is approximately 4-fold higher than our value of 0.256 mM. For the reaction with $EtO_2H$, our value of $k_{obs}^{max}$ is 156 s$^{-1}$, while theirs is 28 s$^{-1}$, and our value of $K_M$ is 2.82 mM, while theirs is 0.71 mM. These are very difficult experiments and the reproducibility is lower than for ambient temperature stopped-flow measurements.

Balny and associates have also reported that the kinetic parameters for the reaction of HRP with both $H_2O_2$ and $EtO_2H$ were strongly dependent on whether the cryosolvent contained DMSO or methanol as the organic cosolvent.[9] Our attempts to repeat their kinetic measurements of the reaction of HRP with $H_2O_2$ and $EtO_2H$ in 60% DMSO/40 mM Tris, pH* 8.7, using [HRP] = 1.0 $\mu$M at subzero temperatures were not successful. Below -10 °C, the kinetic traces started to change abruptly and the sign of all absorbance changes were negative, regardless of the wavelength used to monitor the reaction. These observations indicated that the absorbance changes being observed were not the result of the compound I formation reaction. This was confirmed in a series of control experiments in which 1.0 $\mu$M HRP was mixed with the identical crysolvent containing no peroxide as a function of temperature over the 0 to -29.0 °C range. The stopped-flow traces for these experiments in 50% v/v methanol/40 mM Tris, pH* 8.7, and 60% v/v DMSO/40 mM Tris, pH* 8.7, and shown in parts A and B of Figure 2, respectively. For the methanol-based cryosolvent, there is no appreciable change in absorbance during these mixing experiments over the entire temperature range studied. In the DMSO-based cryosolvent used by Balny and associates, however, an apparent absorbance decrease is observed during this dilution experiment at temperatures below -10 °C. The amplitude and half-life of this signal increases as the temperature is lowered to -24 °C, and the sign of this change is always negative, regardless of the wavelength at which the reaction is monitored (data not shown). Thus, this signal is an
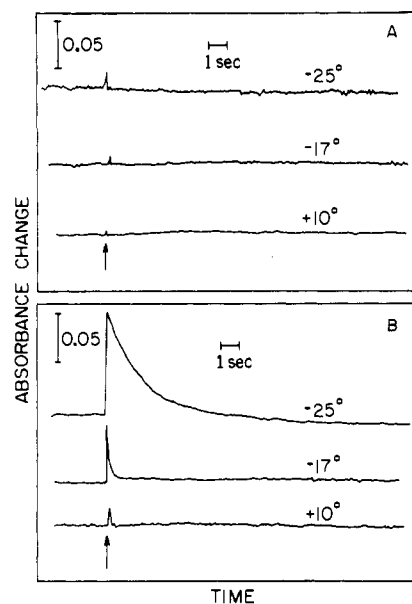


**Figure 2.** Low-temperature stopped-flow traces showing the absorbance change at 397 nm on mixing cryosolvent with 1.0 $\mu$M HRP dissolved in the identical cryosolvent at the temperatures indicated, where the cryosolvent was (A) 50% v/v methanol/40 mM Tris, pH* 8.7, and (B) 60% v/v DMSO/40 mM Tris, pH* 8.7.

artifact caused by the use of DMSO, perhaps due to aggregation of HRP in this crysolvent at lower temperatures. Thus, in all of the experiments described below, only 50% v/v methanol/10 mM phosphate was used as the cryosolvent.

**Effect of Temperature on the Rate of Formation of Compound I.** Values of $k_{obs}$ for the reaction of HRP with 0.30 mM $EtO_2H$, 12.5 mM $t$-$BuO_2H$, and 25 $\mu$M $AcO_2H$ to form compound I have been measured over the +22 to -31 °C temperature range in 50% v/v methanol/10 mM phosphate, pH* 7.3, hereafter referred to as cryosolvent, under pseudo-first-order conditions. At these peroxide concentrations, $k_{obs}$ is first order in peroxide and reflects the $k_{obs}^{max}/K_M$ value for each reaction (see below). The values of $k_{obs}^{max}/K_M$ for the reactions decrease in the order $H_2O_2$ > $AcO_2H$ > $EtO_2H$ > $t$-$BuO_2H$ at all temperatures studied. At approximately -26.2 °C, the values of $k_{obs}^{max}/K_M$ for these reactions are 858, 96.3, 82.3, and 0.415 mM$^{-1}$ s$^{-1}$, respectively.

Arrhenius plots constructed from these data are shown in Figure 3. The data reported earlier[8] for $H_2O_2$ are also shown for comparison. The linearity of these plots indicates that there is no change in the rate-determining step of the reaction or conformational change in HRP that affects its catalytic efficiency over the entire temperature range studied. Thus, the overall reduction in rate is simply attributable to the lowered temperature. Values of $E_a$ have been calculated from Arrhenius plots, and values of $\Delta H^\ddagger$ and $\Delta S^\ddagger$ have been calculated from plots of ln ($k_{obs}/T$) vs $1/T$[20] using data over the temperature range of -4.6 to -36.0 °C

(20) Amdur, I.; Hammes, G. G. Chemical Kinetics: Principles and Selected Topics; McGraw-Hill: New York, 1966; pp 53–58.

*Mechanism of Formation of Compounds 0 and I*

*J. Am. Chem. Soc., Vol. 114, No. 2, 1992* 721
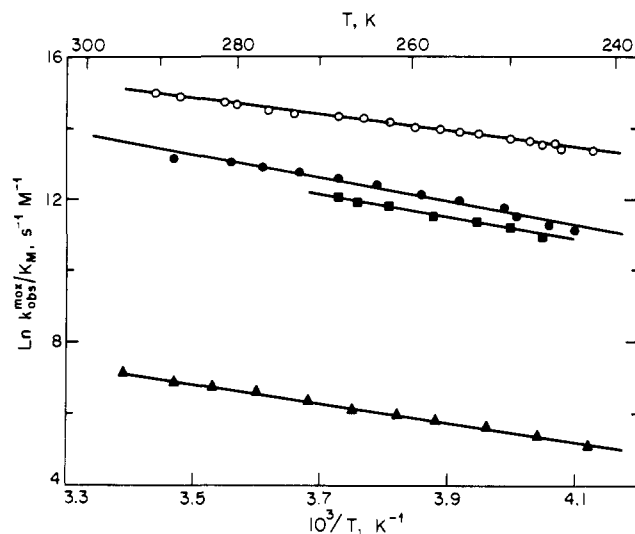


**Figure 3.** Arrhenius plots for the reaction of 1 $\mu$M HRP with (O) 12.5 $\mu$M $H_2O_2$, (■) 0.30 mM $EtO_2H$, (▲) 12.5 mM $t$-$BuO_2H$, and (●) 25 $\mu$M $AcO_2H$ to form compound I in 50% v/v methanol/10 mM phosphate, pH* 7.3.

**Table II.** Thermodynamic Activation Parameters for the Pseudo-First-Order Rate Constant for the Reaction of HRP with Various Peroxides To Form Compound I[a]

| peroxide | $E_a$ (kcal/mol) | $\Delta S^\ddagger$ (eu) | $\Delta H^\ddagger$ (kcal/mol) |
|---|---|---|---|
| $H_2O_2$ | 5.4 ± 0.8 | −12 ± 2 | 4.8 ± 0.8 |
| $EtO_2H$ | 6.3 ± 0.7 | −13 ± 3 | 5.8 ± 0.9 |
| $t$-$BuO_2H$ | 5.5 ± 0.8 | −28 ± 2 | 5.0 ± 0.8 |
| $AcO_2H$ | 8.0 ± 1.2 | −5 ± 4 | 7.4 ± 1.2 |

[a] All reactions were carried out in 50% v/v methanol/10 mM phosphate, pH* 7.3, under conditions where [peroxide] $\ll K_M$ and $k_{obs}$ reflects $k_{obs}^{max}/K_M$. Data in the −4.6 to −36.0 °C temperature range were used for the calculations.

(Table II). The values of $\Delta H^\ddagger$ fall in the 4.8–7.4 kcal/m range and do not differ appreciably for the reactions with the four peroxides. The values of $\Delta S^\ddagger$ are all large and negative. Their magnitudes are very similar for $H_2O_2$, $EtO_2H$, and $AcO_2H$ (−5 to −13 eu), but much more unfavorable (−28 eu) for $t$-$BuO_2H$. Thus, the relative rates of the compound I formation reaction as reflected by $k_{obs}^{max}/K_M$ values for the four peroxides are determined by both the individual values of $\Delta H^\ddagger$ and $\Delta S^\ddagger$, and no generalizations are obvious.

**Effect of Peroxide Concentration on the Rate of Formation of Compound I.** Values of $k_{obs}$ for the reaction of HRP with all three peroxides to form compound I have been measured as a function of [peroxide] at various subzero temperatures in the cryosolvent. Representative data for $EtO_2H$ are shown in Figure 4A. Above 0 °C, the value of $k_{obs}$ for all three reactions varies approximately linearly with [peroxide] up to the maximum measurable value (data not shown). However, as the temperature is progressively lowered, these plots start to exhibit the saturation behavior observed earlier for the reaction with $H_2O_2$.[8] This behavior is consistent with a preequilibrium mechanism of the following general form

$$\text{HRP} + \text{RO}_2\text{H} \underset{k_{-1}}{\overset{k_1}{\rightleftharpoons}} \text{intermediate} \xrightarrow{k_2} \text{I} \qquad (1)$$
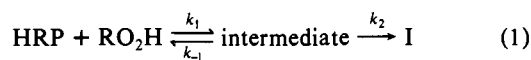
where

$$k_{obs} = \frac{k_{obs}^{max}[\text{RO}_2\text{H}]}{[\text{RO}_2\text{H}] + K_M} \qquad (2)$$

in which $K_M = (k_{-1} + k_2)/k_1$ and is the apparent dissociation constant of the intermediate and $k_{obs}^{max} = k_2$, the rate of conversion of the intermediate to compound I. The observation that all of these plots of $k_{obs}$ vs [RO$_2$H] intersect at the origin confirms that
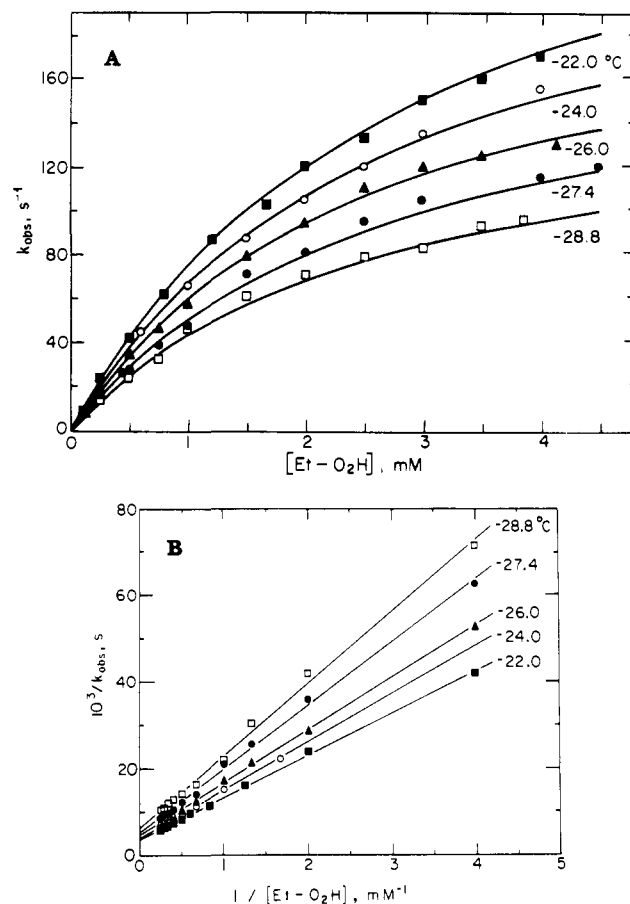


**Figure 4.** (A) Variation in $k_{obs}$ for the reaction of $EtO_2H$ with 1.0 $\mu$M HRP to form compound I in 50% v/v methanol/10 mM phosphate, pH* 7.3, as a function of the concentration of $EtO_2H$ at the temperatures indicated. (B) Double reciprocal plots of the data shown for $EtO_2H$ in (A).

**Table III.** Kinetic Parameters for Reaction of HRP with Peroxides To Form Compound I[a]

| peroxide | $T$ (°C) | $k_{obs}^{max}$ (s$^{-1}$) | $K_M$ (mM) | $k_{obs}^{max}/K_M$ (mM$^{-1}$ s$^{-1}$) |
|---|---|---|---|---|
| $EtO_2H$ | −22.0 | 300 | 3.00 | 100 |
| | −24.0 | 257 | 2.85 | 90.2 |
| | −26.0 | 218 | 2.65 | 82.3 |
| | −27.4 | 191 | 2.79 | 68.5 |
| | −28.8 | 157 | 2.61 | 60.2 |
| $t$-$BuO_2H$ | −20.0 | 112 | 188 | 0.596 |
| | −22.4 | 89.3 | 164 | 0.545 |
| | −24.0 | 63.7 | 135 | 0.472 |
| | −26.2 | 44.8 | 108 | 0.415 |
| | −28.4 | 28.2 | 78.9 | 0.357 |
| $AcO_2H$ | −22.0 | 194 | 1.34 | 188 |
| | −24.0 | 160 | 1.33 | 120 |
| | −26.2 | 130 | 1.35 | 96.3 |
| | −28.0 | 108 | 1.41 | 76.6 |
| | −30.0 | 89.3 | 1.69 | 52.8 |

[a] All reactions were carried out in 50% v/v methanol/10 mM phosphate, pH* 7.3.

all of the compound I formation reactions are irreversible and justifies the omission of $k_{-2}$ in eq 1. Double reciprocal plots of $1/k_{obs}$ vs $1/[\text{peroxide}]$ have been constructed from data at all temperatures where measurements at [peroxide] $\geq K_M$ could be achieved, as shown in Figure 4B for $EtO_2H$, and values of $k_{obs}^{max}$ and $K_M$ have been evaluated (Table III). A comparison of these parameters for these three peroxides and $H_2O_2$[8] near −26 °C shows that $k_{obs}^{max}$ varies from only 44.8 to 218 s$^{-1}$, but that the values of $K_M$ increase with the size of R in RO$_2$H. Specifically, the values are 0.190, 1.35, 2.65, and 108 mM for R = H, Ac, Et, and $t$-Bu, respectively.
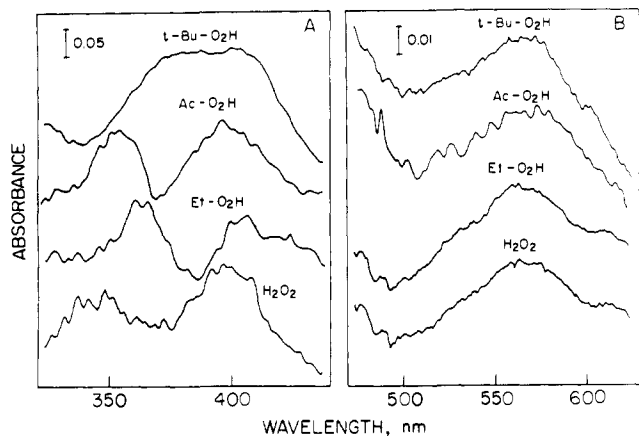
**Figure 5.** Rapid-scan optical spectra (20-ms acquisition time) of the reaction of (A) 1 $\mu$M (Soret region) and (B) 7 $\mu$M (visible region) HRP with 1.0 mM $H_2O_2$, 4.5 mM $EtO_2H$, 3.0 mM $AcO_2H$, and 150 mM $t$-BuO$_2$H in 50% v/v methanol/10 mM phosphate, pH* 7.3, at −35 °C.

As observed earlier for the reaction with $H_2O_2$,[8] the saturation kinetic behavior observed in Figure 4 is a reflection of the change in reaction order with respect to peroxide predicted from eq 2 when the [peroxide] approaches and exceeds $K_M$. HRP recovered from reactions carried out at [peroxide] in the saturation region at these temperatures was found to retain full activity in conventional assays. Thus, the leveling off of $k_{obs}$ at high [peroxide] is not due to damage to the enzyme brought about by the peroxide. In all of these reactions, rapid-scan studies (see below) showed that all of the HRP was fully converted to compound I with the correct spectral properties. The ability to observe saturation kinetics at subzero temperatures is the consequence of the overall lowering of $k_{obs}$ for this reaction, thus enabling the use of a [peroxide] that exceeds $K_M$. The observation of saturation kinetics constitutes direct evidence for a reversible step in the catalytic pathway and points to a mechanism of the type shown in eq 1 with one or more intermediates.

**Direct Observation of the New Intermediate Whose Conversion to Compound I is Rate Limiting.** If it is assumed that a single intermediate accumulates and that it is in a steady state with the reactants, then the fraction of HRP present as the intermediate is given by

$$\frac{[\text{intermediate}]}{[\text{HRP}]} = \frac{[\text{peroxide}]}{[\text{peroxide}] + K_M} \quad (3)$$

and its half-life will be $t_{1/2} \geq (k_{obs}^{max})^{-1}$. Rapid-scan stopped-flow experiments of the reaction of HRP with saturating concentrations of all three peroxides have been carried out in the cryosolvent, pH* 7.3, at −35 °C in order to observe the optical spectrum of the intermediate. Separate experiments have been carried out to record the Soret and visible regions of the spectra using 1.0 and 7.0 $\mu$M HRP, respectively. Since the visible region of the optical spectrum of the intermediate in the reaction with $H_2O_2$ was not recorded earlier, it has also been examined here.

The first (20 ms) scans recorded in the Soret and visible regions after initiation of the reaction with $H_2O_2$ (1.0 mM), $AcO_2H$ (3.0 mM), $EtO_2H$ (4.5 mM), and $t$-BuO$_2$H (150 mM) are shown in parts A and B of Figure 5, respectively. The Soret region for the reaction with $H_2O_2$ exhibits absorption bands near 340 and 400 nm and is very similar to the spectrum observed earlier.[8] The first scan in the reactions with each of the other three peroxides also exhibits two bands, but with different positions and intensities. The spectrum for $AcO_2H$ is closest to that for $H_2O_2$ with nearly equally intense bands at 350 and 400 nm. On going first to $EtO_2H$ and then to $t$-BuO$_2$H, however, the shorter wavelength band shifts to 370 and then to 380 nm, respectively, while the longer wavelength band remains centered near 400–410 nm. In subsequent scans, the shorter wavelength band disappears in all four reactions and is accompanied by a parallel increase in the ~410-nm band characteristic of compound I. The shorter wavelength band is
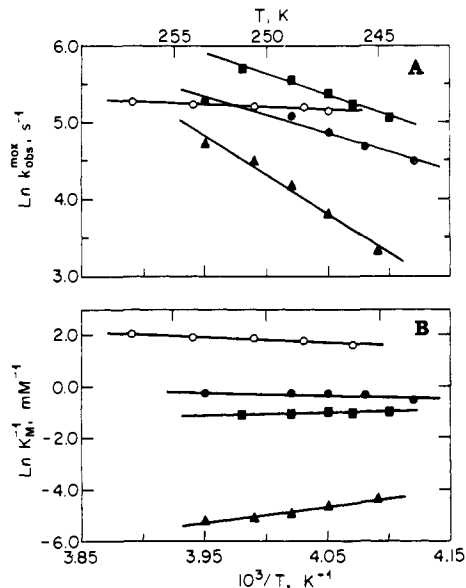


**Figure 6.** (A) Arrhenius plots for $k_{obs}^{max}$ and (B) van't Hoff plots for $K_M^{-1}$ for the reactions of HRP with (O) $H_2O_2$, (■) $EtO_2H$, (▲) $t$-BuO$_2$H, and (●) $AcO_2H$ to form compound I in 50% v/v methanol/10 mM phosphate, pH* 7.3.

**Table IV.** Kinetic Activation Parameters for $k_{obs}^{max}$ Which Describe the Conversion of Compound 0 to Compound I during the Reaction of HRP with Various Peroxides[a]

| peroxide | $E_a$ (kcal/mol) | $\Delta H^{\ddagger}$ (kcal/mol) | $\Delta S^{\ddagger}$ (eu) |
|---|---|---|---|
| $H_2O_2$ | 1.6 ± 0.7 | 1.0 ± 0.2 | −43 ± 3 |
| $EtO_2H$ | 11 ± 1 | 10 ± 1 | −6 ± 1 |
| $t$-BuO$_2$H | 20 ± 3 | 20 ± 3 | +28 ± 6 |
| $AcO_2H$ | 9 ± 2 | 9 ± 2 | −12 ± 10 |

[a] All reactions were carried out in 50% v/v methanol/10 mM phosphate, pH* 7.3, over the −20.0 to −30.0 °C range.

clearly due to the new intermediate. However, because of the short half-life of the new intermediate relative to the mixing and acquisition times, it cannot be established with certainty whether the band near 400–410 nm is due to it or to some compound I that is formed. The visible region shows only a weak, broad band near 570 nm that is almost the same for the intermediates in all four reactions. The spectral features noted above for these reactions are not observed in control experiments involving the mixing of buffer with buffer, buffer with peroxide, or buffer with HRP. These experiments indicate that a compound 0 type reaction intermediate precedes the formation of compound I in the reaction of HRP with all four of these peroxides.

**Temperature Dependence of $k_{obs}^{max}$ and $K_M$.** Arrhenius plots of ln $k_{obs}^{max}$ vs $T^{-1}$ for the three peroxides covering the −20.0 to −30.0 °C range (Table III) are shown in Figure 6A. From these data, values of $E_a$, $\Delta H^{\ddagger}$, and $\Delta S^{\ddagger}$ have been calculated for $k_{obs}^{max}$ as described earlier and the results summarized in Table IV. Values of these parameters for the reaction with $H_2O_2$ are also shown for reference. It can be seen that the values of both $\Delta H^{\ddagger}$ and $\Delta S^{\ddagger}$ vary markedly for these four peroxides. The value of $\Delta H^{\ddagger}$ increases between 9- and 20-fold on going from $H_2O_2$ to the other peroxides. This endows the latter three reactions with a more marked temperature dependence of $k_{obs}^{max}$. The value of $\Delta S^{\ddagger}$ is large and negative (−43 eu) for $H_2O_2$, but is increasingly more positive for the reactions with $AcO_2H$, $EtO_2H$, and $t$-BuO$_2$H. The result of the trends in the $\Delta H^{\ddagger}$ and $\Delta S^{\ddagger}$ values on going from $H_2O_2$ to the other peroxides is a compensation effect in which increasingly positive $\Delta H^{\ddagger}$ values are offset by increasingly positive $\Delta S^{\ddagger}$ values. The net effect is that $k_{obs}^{max}$ varies relatively little (less than 5-fold) for the four peroxides.

$K_M^{-1}$ is the apparent association constant for compound 0 and equals the steady-state concentration of compound 0 divided by the free concentrations of HRP and peroxide. Plots of ln $K_M^{-1}$ vs

**Table V.** Thermodynamic Parameters for the $K_M^{-1}$ Value That Describes the Formation of Compound 0 on Reaction of HRP with Different Peroxides[a]

| peroxide | $\Delta H_0$ (kcal/mol) | $\Delta S_0$ (eu) | $\Delta G_0$ (kcal/mol) | $K_M^{-1}$ ($M^{-1}$) |
|---|---|---|---|---|
| $H_2O_2$ | $4.0 \pm 0.7$ | $33 \pm 3$ | $-4.2 \pm 0.4$ | 5300 |
| $EtO_2H$ | $-2.2 \pm 1.4$ | $3.0 \pm 0.3$ | $-2.9 \pm 0.3$ | 380 |
| $t$-$BuO_2H$ | $-13 \pm 2.0$ | $-46 \pm 5$ | $-1.1 \pm 0.2$ | 9.3 |
| $AcO_2H$ | $2.4 \pm 2.0$ | $23 \pm 10$ | $-3.2 \pm 0.4$ | 740 |

[a] All reactions were carried out in 50% v/v methanol/10 mM phosphate, pH* 7.3, over the $-20.0$ to $-30.0$ °C range. The values of $K_M^{-1}$, $\Delta G_0$, and $\Delta S_0$ are for $-26.0$ °C.

$T^{-1}$ have been constructed (Figure 6) and used to calculate $\Delta H_0$, the enthalpy change associated with the *formation* of compound 0 in the steady state from HRP and peroxide. The $K_M^{-1}$ values at $-26.0$ °C (Table III) have been used to calculate the values of $\Delta G_0$ for these reactions. Using these $\Delta G_0$ values and the $\Delta H_0$ values obtained from the van't Hoff plots, $\Delta S_0$ values for the formation of compound 0 have also been calculated for all four reactions at $-26.0$ °C (Table V). The $\Delta G_0$ values for formation of compound 0 vary from $-1.1$ to $-4.2$ kcal/m, with the reaction more favorable for the smaller peroxides. The values of $\Delta H_0$ and $\Delta S_0$ vary markedly for the different peroxides. The value of $\Delta H_0$ is positive for $H_2O_2$, but decreases markedly and becomes negative on going from $AcO_2H$ to $EtO_2H$ to $t$-$BuO_2H$. The positive values of $\Delta H_0$ for $H_2O_2$ and $AcO_2H$ mean that the formation of compound 0 is an *uphill process* in the catalytic pathway for these smaller peroxides. Surprisingly, the formation of compound 0 is enthalpically *more favorable* for the bulkier peroxides. The value of $\Delta S_0$ also decreases markedly for the bulkier peroxides in the same order as observed for $\Delta H_0$. These decreases more than offset the lower $\Delta H_0$ values and lead to the net increases in $\Delta G_0$ and, thus, the observed decreases in $K_M^{-1}$. The parameters measured for the overall compound I formation reaction (Table II) pertain to $k_{obs}^{max}/K_M$ values and are related to the parameters for the two-step preequilibrium mechanism (eq 1) by the following relationships:

$$\Delta H^\ddagger (k_{obs}^{max}/K_M) = \Delta H_0 + \Delta H^\ddagger (k_{obs}^{max}) \quad (4)$$

$$\Delta S^\ddagger (k_{obs}^{max}/K_M) = \Delta S_0 + \Delta S^\ddagger (k_{obs}^{max}) \quad (5)$$

The sum of the values of the two parameters on the right-hand side of each of these equations (Tables IV and V) agrees within experimental error with the value on the left-hand side for each peroxide when data over the same temperature ranges ($-20$ to $-30$ °C) are compared.

## Discussion

The low-temperature stopped-flow data presented here and in a previous study[8] show that the reaction of HRP with several peroxides in 50% v/v methanol/10 mM phosphate at subzero temperatures exhibits saturation kinetics. There is no evidence that the 50% v/v methanol-based cryosolvent or subzero temperatures used in this study alter the fundamental nature of the reaction in any way, other than to reduce the magnitudes of the rate constants for the elementary steps. Saturation kinetic data for the reaction of HRP with $H_2O_2$ and $EtO_2H$ in a similar 50% v/v methanol-based crysolvent have also been reported by other researchers.[9] The agreement between the kinetic parameters $k_{obs}^{max}$ and $K_M$ for these reactions and ours is only fair, and the discrepancies do not appear to be related to the buffering ion, pH*, or [HRP] employed (Table I). However, considering the difficulties of such experiments, some disagreements are to be expected, particularly if these parameters are derived from data sets for which [peroxide]$_{max}$ < $K_M$.[9] These same researchers also studied these reactions in a 60% v/v DMSO-based cryosolvent and found markedly different kinetic parameters than in the methanol-based cryosolvent. The data presented here, however, indicate that the 60% v/v DMSO-based cryosolvent is not suitable for studying these reactions by the low-temperature stopped-flow technique, casting doubt on the validity of the kinetic parameters reported.

The saturation kinetics data reported here and earlier[8] confirm the hypothesis of Jones and Dunford[4] that the minimum acceptable mechanism for compound I formation for HRP involves at least one reversible step. Rapid-scan studies with the three peroxides used here show that the species whose conversion to compound I is rate limiting has an optical spectrum that is similar to that found earlier for the reaction with $H_2O_2$.[8] Thus, a compound 0 type species is apparently a common intermediate in all four reactions. Another consideration pertinent to the kinetic pathway of compound I formation is that the initial step in the interaction between an alkyl hydroperoxide and a ferric heme species is widely believed to be the formation of an $Fe(III)(^-O_2R)$ precursor complex. HRP itself is known to bind the neutral form of acid ligands.[1] By analogy to the binding of $HCN$,[21] $RO_2H$ is envisaged to bind to HRP via entry of the unionized peroxide into the active site with a subsequent concerted formation of the ferric hydroperoxy anion complex and transfer of the hydroperoxide proton to the neutral distal His-42 residue, converting it to the imidazolium form. Thus, it seems overwhelmingly likely that such a precursor complex is the first intermediate in the reaction pathway of HRP and $RO_2H$ to form compound I, as proposed for cytochrome c peroxidase.[22] Assuming that compound 0 is not identical with this complex (see below), the simplest mechansim consistent with the existence of both intermediates is

$$HRP + RO_2H \underset{k_{-1}}{\overset{k_1}{\rightleftharpoons}} ((HRP)H^+)(^-O_2R) \underset{k_{-2}}{\overset{k_2}{\rightleftharpoons}} 0 \overset{k_3}{\longrightarrow} I \quad (6)$$

where $((HRP)H^+)(^-O_2R)$ is a precursor complex that is a protonated form of HRP containing $RO_2^-$ as the distal ligand to the $Fe(III)$ atom of the heme group. Steps 1 and 2 are not resolved in our experiments, and step 3 is rate limiting. Thus, mechanism 6 reduces to mechanism 1 with intermediate = compound 0, where the relationship between parameters is

$$k_{obs}^{max} = k_2 k_3/(k_2 + k_{-2}) \quad (7)$$

$$K_M = [k_{-2}/(k_2 + k_{-2})]K_S \quad (8)$$

where $K_S = k_{-1}/k_1$.[23]

In the context of the two-step formation of compound I (eq 1), $K_M^{-1}$ is the apparent formation constant for compound 0 from free HRP and free $RO_2H$, $k_{obs}^{max}$ is a first-order rate constant that describes its conversion to compound I, and $k_{obs}^{max}/K_M$ is the apparent second-order rate constant for compound I formation from free HRP and free $RO_2H$. The trends in these kinetic parameters and the thermodynamic parameters derived from them (Tables II–V) provide insights into the catalytic pathway for the reaction of HRP with the four peroxides studied. Starting with the data for the overall reaction at $-26$ °C, the $k_{obs}^{max}/K_M$ values are 858, 96.3, 82.3, and 0.415 mM$^{-1}$ s$^{-1}$ for $H_2O_2$, $AcO_2H$, $EtO_2H$, and $t$-$BuO_2H$, respectively. The data in Table II indicate that neither the $\Delta H^\ddagger$ nor $\Delta S^\ddagger$ values that describe the overall compound I formation reaction play a dominant role in determining the relative value of $k_{obs}^{max}/K_M$.

The thermodynamic parameters that describe the formation of compound 0 (Table V) and the kinetic activation parameters that describe its conversion to compound I (Table IV), however, show more clearly pronounced trends. The formation of compound 0 is enthalpically unfavorable for $H_2O_2$, but becomes more favorable as the size of the substituent (R) on the peroxide increases. Conversely, compound 0 formation is entropically the most favorable for $H_2O_2$ and becomes less favorable for the larger peroxides. The net result is a compensation effect on $\Delta G_0$. Since the decreases in $\Delta S_0$ are the larger effects, they lead to more positive values of $\Delta G_0$ and smaller values of $K_M^{-1}$ for the larger peroxides. It is not immediately clear why the formation of HRP compound 0 in the reaction with $H_2O_2$ is enthalpically unfavorable

(21) Thanabal, V.; de Ropp, J. S.; La Mar, G. N. *J. Am. Chem. Soc.* **1988**, *110*, 3027.

(22) Poulos, T. L.; Kraut, J. *J. Biol. Chem.* **1980**, *255*, 8199.

(23) Bernasconi, C. F. *Relaxation Kinetics*; Academic: New York, 1976; p 45.

724 *J. Am. Chem. Soc., Vol. 114, No. 2, 1992*

*Baek and Van Wart*

and entropically driven. The positive $\Delta H_0$ value and unusual optical spectrum of compound 0 suggest that some electron transfer between $H_2O_2$ and the heme group has occurred through kinetic channeling to produce this metastable intermediate. Given this, the trends in $\Delta G_0$ and $\Delta S_0$ on going to the bulkier $RO_2H$ are consistent with the R substituent being retained in compound 0. Thus, the fact that the bulkier peroxides have more positive $\Delta G_0$ values and lower values of $K_M^{-1}$ is consistent with the notion that the R group is still present in compound 0. The more negative values of $\Delta S_0$ for the larger peroxides are consistent with the greater losses in freedom expected when they are brought into the active site of HRP. With regard to the more favorable $\Delta H_0$ values for the bulkier peroxides, it is difficult to envision this as arising from favorable interactions with the active site. Instead, it seems more likely that the trends in $\Delta H_0$ are related to their relative enthalpies of transfer out of aqueous solution and to differences associated with the oxidation that appears to be associated with the formation of compound 0.

The activation parameters $\Delta H^{\ddagger}$ and $\Delta S^{\ddagger}$ that describe the conversion of compound 0 to compound I for $H_2O_2$ and the changes in these parameters for the reactions with the bulkier peroxides are also very interesting. For $H_2O_2$, $\Delta H^{\ddagger}$ is small (1.0 kcal/mol), but increases 9- to 20-fold for $RO_2H$. The $\Delta S^{\ddagger}$ for $H_2O_2$ is extremely unfavorable, but becomes much more positive on going from $AcO_2H$ to $EtO_2H$ to $t$-$BuO_2H$. The low value of $k_{obs}^{max}$ for the reaction with $H_2O_2$ in spite of the low $\Delta H^{\ddagger}$ is the result of the very unfavorable $\Delta S^{\ddagger}$ value. This is indicative of a step with a high Franck–Condon barrier, or one that is otherwise forbidden for reasons having to do with orbital symmetry or overlap.[24] The changes in $\Delta H^{\ddagger}$ and $\Delta S^{\ddagger}$ observed for the other $RO_2H$ may be the result of superimposing other effects on this basic reaction. The steplike increase in $\Delta H^{\ddagger}$ on going from $HO_2H$ to the other $RO_2H$ suggests that the replaced H atom plays a specific role in facilitating attainment of the transition state for $H_2O_2$. The fact that $\Delta S^{\ddagger}$ is more positive for the bulkier $RO_2H$ is also consistent with the notion that the R substituent is still present in compound 0, since its release on conversion to compound I would account for this trend.

The optical spectrum of compound 0 can, in principle, provide important clues to its identity. It is, unfortunately, very difficult to clearly distinguish which features in the optical spectra of the reaction mixtures arise from compound 0 vs those that arise from compound I. As observed earlier for the reaction with $H_2O_2$, the Soret region is characterized by bands near 360 and 400 nm.[8] Both bands could be attributable to compound 0, in which case it would have a "hyperporphyrin" type spectrum with a split Soret band.[26] Alternatively, the possibility that compound 0 contributes only the band near 360 nm and that the band near 400 nm is due to some compound I that has formed during the time period of the scan cannot be ruled out. It is significant that the position of the band near 360 nm depends upon the identity of the $RO_2H$ used in the reaction, supporting the view that R is retained in compound 0. If the compound 0 species formed on reaction with each peroxide had identical structures, all should exhibit the same optical spectra. In the visible region, compound 0 exhibits only a weak featureless band centered near 570 nm for all four peroxides.

More detailed spectroscopic studies of compound 0 will be required to establish its structure. However, the kinetic, ther-
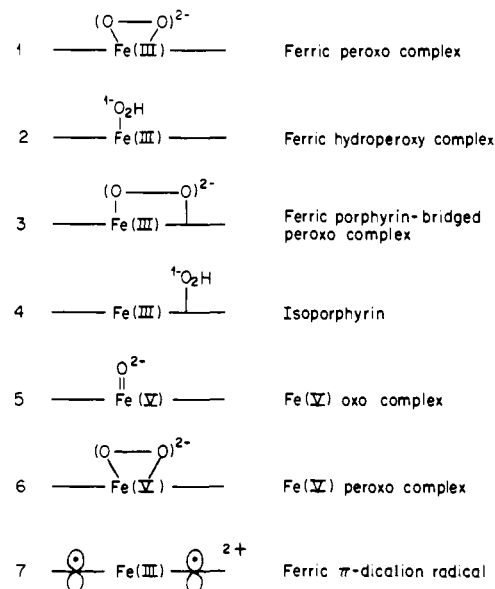


**Figure 7.** Schematic illustration of possible structures for compound 0. The horizontal line represents the porphyrin ring.

modynamic, and optical data discussed above are helpful in distinguishing between several alternatives. After the initial discovery of compound 0 in the reaction of HRP with $H_2O_2$, several candidate structures were delineated by considering potential interactions between $H_2O_2$ and the heme group.[8] Seven such species are shown schematically in Figure 7. Species 1 and 2 are true precursor complexes in which doubly and singly ionized $H_2O_2$ coordinate to Fe(III), respectively, while 3 has the peroxo group bridged between Fe(III) and an unspecified porphyrin atom (e.g., a pyrrole nitrogen to form an $N$-peroxo heme). In species 4, the $O_2H$ group is bound at a methine carbon to give an isoporphyrin. In species 5–7, the iron atom or porphyrin ring has been oxidized by two electrons and one (5) or both (6, 7) of the oxygen atoms of the *original* $H_2O_2$ oxidant have been lost. Species 6 is an intermediate that could be formed from 5 by exchange of its oxo ligand by the peroxo group of a second $H_2O_2$ molecule. The rationale for considering it is that if 5 were the true intermediate formed at low [$H_2O_2$], it could be converted to 6 at the high [$H_2O_2$] used to observe compound 0, where it could serve to better stabilize the Fe(V) state.[25]

On the basis of the observation in this study that all three $RO_2H$ produce a compound 0 similar to that obtained with $H_2O_2$, species 1, 3, and 6 can be eliminated, since their formation would require scission of the $R$–$O_2H$ bond. Similar species in which there were coordination of both oxygen atoms of $RO_2^-$ to the iron atom, however, remain possibilities. Of the remaining species, 2 and 4 both contain the R group of the original peroxide, while 5 and 7 do not. While the $K_M^{-1}$ and $\Delta S_0$ values for compound 0 formation and the $\Delta H^{\ddagger}$ and $\Delta S^{\ddagger}$ values for $k_{obs}^{max}$ all seem to imply that the RO group of $RO_2H$ has been retained in compound 0, its optical spectrum is inconsistent with that expected for species 2. The spectrum of the ferric hydroperoxy complex (2) should resemble that of $(TMP)Fe(III)(t$-$BuO^-_2)$[27] or other ferric–oxyanion complexes[28] that have relatively normal Soret- and Q-band spectra. Isoporphyrins such as 4 do exhibit absorption bands in the 360-nm region as well as a characteristic doublet near 800–900 nm,[29–32]

(24) Katakis, D.; Gordon, G. *Mechanisms of Inorganic Reactions*; John Wiley & Sons, Inc.; New York, 1987.

(25) This would mean that there is a change in mechanism at high [$H_2O_2$] involving a second molecule of $H_2O_2$. If its interaction with 5 to form 6 was faster than the rate of conversion of 6 to compound I, and if 5 and 6 converted to compound I at equal rates, this change in mechanism would be kinetically invisible. Since the peroxo group of 6 would have to dissociate and be replaced by an oxo group that would likely be derived from water before conversion to compound I, however, this would provide a test for the presence of such a species. Experiments carried out at high [$H_2^{18}O_2$] in $H_2^{16}O$ would give Fe(IV)=$^{16}O$ in compound I rather than the Fe(IV)=$^{18}O$ found when carried out at low [$H_2^{18}O_2$].

(26) Gouterman, M. In *The Porphyrins*; Dolphin, D., Ed.; Academic: New York, 1978; Vol. III, pp 1–166.

(27) Arasasingham, R. D.; Cornman, C. R.; Balch, A. L. *J. Am. Chem. Soc.* **1989**, *111*, 7800.

(28) Burstyn, J. N.; Roe, J. A.; Mikzstal, A. R.; Shaevitz, B. A.; Lang, G.; Valentine, J. S. *J. Am. Chem. Soc.* **1988**, *110*, 1382.

(29) Gold, A.; Ivey, W.; Toney, G. E.; Sangaiah, R. *Inorg. Chem.* **1984**, *23*, 2932–2935.

(30) Dolphin, D.; Felton, R. H.; Borg, D. C.; Fajer, J. J. *J. Am. Chem. Soc.* **1970**, *92*, 743.

(31) Dolphin, D.; Halko, D. J.; Johnson, E. C.; Rousseau, K. In *Porphyrin Chemistry Advances*; Longo, F. R., Ed.; Ann Arbor Science: Ann Arbor, 1977; p 119.

as observed for the 5-butyl hydroperoxy adduct of tetrakis(4-methoxyphenyl) iron(III) porphyrin.[29] The latter region has not yet been studied carefully for compound 0 and should be diagnostic for this type of species.

Turning attention to species **5**, an iron(V) porphyrin similar to the p-type manganese(III) hyperporphyrins should have a number of sharp, well-defined bands in the 500–800-nm region.[22] These are not observed for compound 0; however, since there is no precedent for species **5**, its optical spectrum would be difficult to predict. Finally, the ferric π-dication radical (7) of the Zn(II) and Mg(II) complexes of OEP exhibit bands near 350 nm in the ultraviolet and have a weak featureless band near 550 nm.[33] These

features are close to those observed for compound 0. However, a structure of this type is hard to rationalize with the thermodynamic and activation parameters unless the RO portion of $RO_2H$ remains bound. One intriguing possibility is that compound 0 is a ferric porphyrin π-dication radical produced by an initial, selective oxidation of the porphyrin ligand and that $k_{obs}^{max}$ reflects its conversion to compound I through an intramolecular electron transfer from the ferric atom to the porphyrin radical. More detailed studies will be required to resolve these questions.

(32) Guzinski, J. A.; Felton, R. J. *J. Chem. Soc., Chem. Commun.* **1973**, 715.

(33) Fajer, J.; Borg, D. C.; Forman, A.; Dolphin, D.; Felton, R. H. *J. Am. Chem. Soc.* **1970**, *92*, 3451.

# Evidence for Temperature-Dependent Changes in the Coupling within the Type 2/Type 3 Cluster of Laccase

Ji-bin Li,[†] David R. McMillin,[*,†] and William E. Antholine[‡]

*Contribution from the Department of Chemistry, Purdue University, 1393 Brown Building, West Lafayette, Indiana 47907-1393, and National Biomedical ESR Center, 8701 Watertown Plank Road, Milwaukee, Wisconsin 53226. Received June 17, 1991*

**Abstract:** The type 2 depleted form of isotopically enriched laccase has been prepared and subsequently reconstituted with a different copper isotope. The results indicate that the copper ion which is removed and reinserted is *not* the same copper ion that is responsible for the type 2 EPR signal observed at low temperature. However, S-band EPR data show that the reactive copper center is EPR active at room temperature. These findings are explained in terms of a temperature-dependent structural reorganization and a change in the nature of the antiferromagnetic coupling that occurs within the type 2/type 3 cluster of laccase. This phenomenon may be connected with a previously identified conformational transition of the enzyme.

## Introduction

The copper-containing proteins laccase, ascorbate oxidase, and ceruloplasmin form a class of enzymes known as the blue oxidases which catalyze the reduction of dioxygen to water without releasing potentially harmful intermediates such as $H_2O_2$ and the hydroxyl radical. A minimum of four copper ions appears to be required for efficient catalysis, and they are distributed in three spectroscopically distinct binding sites.[1,2] The type 1, or blue, copper center gives rise to an EPR signal and exhibits a strong visible absorbance near 600 nm that is responsible for the enzyme's blue color. The type 2 copper is also EPR active, but as yet no absorption bands have been resolved for this site. In contrast, the pair of coppers bound in the type 3 site exhibit absorption bands in the visible[3] and near-ultraviolet, but they are EPR silent due to a strong antiferromagnetic coupling interaction. Of all the blue oxidases, laccase is probably the easiest to investigate from the mechanistic viewpoint because in this enzyme each type of copper-binding site occurs only once. However, ascorbate oxidase, which contains two copies of each site, has been crystallographically characterized.[4]

Chemical modification studies have contributed to our understanding of laccase, and the preparation of the type 2 depleted (T2D) form of tree laccase can be considered to be a hallmark in the modification work.[5-7] T2D laccase contains three coppers and when oxidized exhibits characteristic spectroscopic signals of the type 1 and type 3 copper sites.[6-8] Evidently, the type 2 copper can be removed without significantly modifying the other

copper sites. However, recent anion-binding studies involving laccase as well as structural studies of ascorbate oxidase suggest that the type 2 and type 3 coppers are so intimately related that they cannot necessarily be construed as separate sites.[4,9,10] Some workers have even speculated that all three of the copper ions within the type 2/type 3 cluster can be magnetically coupled.[11,12] The isotope-labeling studies described below provide striking new evidence of cooperative interactions within the cluster.

## Experimental Section

**Materials.** Acetone powder of the latex of the Chinese lacquer tree (*Rhus vernicifera*) was harvested near Chu Shi, China, and supplied by Saito and Co., Osaka, Japan. Laccase was extracted and purified by the method of Reinhammar.[13] Isotopically pure $^{63}CuO$ and $^{65}CuO$ were

* To whom correspondence should be addressed.
† Purdue University.
‡ National Biomedical ESR Center.

(1) Fee, J. A. *Struct. Bonding (Berlin)* **1975**, *23*, 1-60.
(2) Reinhammar, B. In *Copper Proteins and Copper Enzymes*; Lontie, R., Ed.; CRC Press: Boca Raton, FL, 1984; Vol. 3, 1-35.
(3) Tamilarasan, R.; McMillin, D. R. *Biochem. J.* **1989**, *263*, 425-429.
(4) Messerschmidt, A.; Rossi, A.; Ladenstein, R.; Huber, R.; Bolognesi, M.; Gatti, G.; Marchesini, A.; Petruzzelli, R.; Finazzi-Agrò, A. *J. Mol. Biol.* **1989**, *206*, 515-529.
(5) Graziani, M. T.; Morpurgo, L.; Rotilio, G.; Mondovì, B. *FEBS Lett.* **1976**, *70*, 87-90.
(6) Morpurgo, L.; Savini, I.; Mondovì, B.; Avigliano, L. *J. Inorg. Biochem.* **1987**, *29*, 25-31.
(7) Klemens, A. S.; McMillin, D. R. *J. Inorg. Biochem.* **1990**, *38*, 107-115.
(8) Kau, L.-S.; Spira-Solomon, D. J.; Penner-Hahn, J. E.; Hodgson, K. O.; Solomon, E. I. *J. Am. Chem. Soc.* **1987**, *109*, 6433-6442.
(9) Spira-Solomon, D. J.; Allendorf, M. D.; Solomon, E. I. *J. Am. Chem. Soc.* **1986**, *108*, 5318-5328.
(10) Severns, J. C.; McMillin, D. R. *Biochemistry* **1990**, *29*, 8592-8597.
(11) Calabrese, L.; Carbonaro, M.; Musci, G. *J. Biol. Chem.* **1989**, *264*, 6183-6187.
(12) Cole, J. L.; Clark, P. A.; Solomon, E. I. *J. Am. Chem. Soc.* **1990**, *112*, 9534-9548.